Influence of Particle Volume Fraction on Packing in Responsive Hydrogel Colloidal Crystals

Saet Byul Debord and L. Andrew Lyon*

Georgia Institute of Technology, School of Chemistry and Biochemistry, Atlanta, Georgia 30332-0400

Received: August 16, 2002; In Final Form: January 15, 2003

We describe the influence of particle concentration on the formation of crystals from soft colloidal particles. Specifically, laser scanning confocal and differential interference contrast microscopies are used to directly observe the packing in entropic crystals formed from submicron-sized particles composed of the thermoresponsive polymer poly-*N*-isopropylacrylamide (pNIPAm) and the thermoresponsive/pH-responsive copolymer poly-*N*-isopropylacrylamide-*co*-acrylic acid (pNIPAm-AAc). Close-packed crystals are observed when either the pNIPAm and pNIPAm-AAc particles are concentrated by centrifugation. At that point the particle−particle spacing is smaller than the hydrodynamic diameter as determined by photon correlation spectroscopy, reflecting compression of the soft particles. Upon dilution of the pNIPAm crystals, the melting point of the assembly is reached when the repulsive particle interactions are no longer sufficient to dictate long-range order in the assembly. However, excellent crystallization is observed even after a 9-fold dilution of the acrylic acid-containing particles, whereupon the particle size and hence the center-to-center particle spacing is observed to be more than twice that of the original sample. These results are not explainable using a simple hard-sphere packing model, which would predict crystal melting upon dilution, and are therefore interpreted in terms of particle compressibility (for higher concentration samples) as well as an attractive pair- or multibody-potential (for low-concentration samples).

Introduction

Predictions that omnidirectional band gaps[1,2] should be observable in opal-inspired materials have stimulated investigations into the materials science and optical physics of self-assembled photonic materials.[3−6] The building blocks for such materials are often spherical colloidal particles, which (as in natural opals)[7,8] assemble into diffractive cubic close-packed structures and hence are excellent templates for the synthesis of slightly more advanced diffractive periodic dielectric structures such as inverse opals.[4,9,10] However, before this relatively recent interest in opaline photonic structures, dispersions and suspensions of spherical colloidal particles had been studied extensively as models for condensed matter phase behavior.[11−14] Just as in molecular systems, colloidal dispersions display gaseous, fluid, crystalline, and glassy phases, with the relevant phase transitions corresponding closely to those transitions observed in molecular assemblies. Although many of these investigations have utilized particles that display interaction potentials that are dominated by hard-sphere repulsion, others have probed the interplay of soft interactions, and the influence of such potentials on the resultant phase diagram.[15−20] Finally, the appearance of attractive interactions (which lead to an unusual fluid/crystal phase coexistence) in systems designed to have purely repulsive interactions have been an area of recent intense interest.[21−25]

In this paper, we describe the phase behavior of aqueous dispersions of spherical, submicron-sized particles composed largely of the thermoresponsive polymer poly-*N*-isopropylacrylamide (pNIPAm).[26−28] Such particles are typically referred to as microgels or hydrogel particles, as pNIPAm is water-soluble at room temperature. Thus, loosely cross-linked particles of the polymer tend to swell dramatically in aqueous media, with the water content often being >95 vol %. As a result of this extreme degree of solvent swelling, such particles might be expected to display a soft interaction potential. Indeed, others have indirectly illustrated the presence of a soft (concentration-dependent) interaction potential in pNIPAm particles and shown the influence of this softness on the crystallization and melting behavior of entropic crystals.[18,29] Of additional interest with respect to these particle assemblies is the thermoresponsivity of pNIPAm. Below its characteristic lower critical solution temperature (LCST) of ∼31 °C, pNIPAm exists as a solvated random coil in aqueous media. However, above that temperature, the chains collapse to a hydrophobic globular state due to the entropically favored release of water from the polymer. For cross-linked microgels, this transition is typically referred to as the volume phase transition (VPT), where the particle undergoes a transition from a swollen to a de-swollen network. Our group has utilized this VPT to create colloidal crystals from pNIPAm particles that are optically tunable by controlling the degree of particle hydration, and crystals that can be annealed via the VPT.[30,31] The studies described below are designed to elucidate the influence of soft *and* weakly attractive particle interactions on the phase behavior of colloidal dispersions. Our results suggest that particles with such unique interaction potentials may offer new opportunities for the construction of periodic, self-assembled structures.

Experimental Section

Materials. *N*-Isopropylacrylamide (NIPAm, Aldrich) was purified by recrystallization from hexane (J. T. Baker) prior to use. Acrylic acid (AAc), *N*,*N*′-methylenebis(acrylamide) (BIS),

* Author to whom correspondence should be addressed. E-mail: lyon@chemistry.gatech.edu.

10.1021/jp026783n CCC: $25.00
Published on Web 03/12/2003

ammonium persulfate (APS), and fluorescein disodium salt were purchased from Aldrich and used as received. Water was purified with Barnstead E-Pure system to a resistance of 18 MΩ.

Particle Synthesis. PNIPAm-AAc particles were prepared as follows. NIPAm (1.4 g) and 0.03 g of cross-linker (BIS) were dissolved in 100 mL of water and filtered to remove particulate matter. The mixture was transferred into a 250 mL round-bottom flask and heated and kept at 70 °C under a gentle nitrogen stream for 40 min. Then, 95 μL of AAc was added, followed by APS (0.05 g) to initiate polymerization. The reaction mixture was kept at 70 °C under nitrogen at least for 4 h to complete the reaction. PNIPAm particles were synthesized by the same method as the pNIPAm-AAc particle preparation. NIPAm (2.0 g) and BIS (0.04 g) were dissolved in 100 mL of water and filtered. The reaction mixture was transferred into a 250 mL round-bottom flask and heated in the same manner as above. APS (0.05 g) was added to initiate reaction. After synthesis, the hydrogel solution was filtered and purified by dialysis (Spectra/Por 7 dialysis membrane, MWCO 10 000) for at least 7 days. The hydrodynamic radius and size distribution of the hydrogel particles were characterized with photon correlation spectroscopy (PCS, Protein Solutions, Inc.) as described previously.[32−34] In general, PCS-determined polydispersities fall below 20%. However, it should be noted that this "effective" polydispersity probably reflects the presence of loosely crosslinked chains at the particle surface, which contribute to the hydrodynamic radius but may not contribute greatly to crystallization, especially at high-volume fractions. Thus, the relationship between PCS-determined polydispersites of hydrogel particles and crystallization thermodynamics/defect density is not clear at this point. Nonetheless, for this and previous studies,[32−34] it has been found that excellent crystallization is observed when the PCS-determined values lie below 20%.

Crystal Assembly. To concentrate the particles into close contact, a hydrogel solution was centrifuged at 29 °C at a relative centrifugal force (RCF) 16 100*g* for 1 h. The ionic strength of the hydrogel solutions was adjusted ∼1 mM with 0.1 M NaCl solution before centrifugation. For samples for confocal microscopic observation, a fluorescein disodium salt solution was added to the sample to a concentration of 2.8×10^{-5} M. After centrifugation, the supernatant water was removed to isolate the particle pellet. Diluted crystal samples were prepared by adding H_2O to the pellet in the centrifuge tube while maintaining the ionic strength of samples at ∼1 mM with a 0.1 M NaCl solution. To control the extent of AAc protonation, the pH of the samples was adjusted to ∼3.8 with 0.01 M HCl. After dilution, the crystals were transferred into Vitrotube borosilicate rectangular capillaries (0.1 mm × 2.0 mm) by capillary action and annealed between room temperature and 35 °C at least 15 times before observation.

Microscopy. Differential interference contrast (DIC) images were taken with an Olympus IX-70 inverted microscope using standard DIC optics. For confocal laser scanning microscopic images, a Leica confocal microscope (Ar^+ laser, 488 nm excitation line) was used. The emission in the range from 500 to 650 nm was used to detect fluorescence from the fluorescein dye.

Results and Discussion

Before discussing the details of the unique particles used in this system, it is worthwhile revisiting the classic case of hard sphere assembly.[14] The basic phase diagram that governs hard sphere behavior is fairly well understood and is illustrated in Scheme 1. This diagram is incomplete in that it does not cover

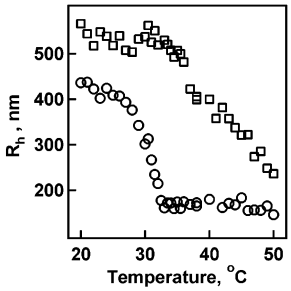

Figure 1. Photon correlation spectroscopy as a function of temperature for pNIPAm-AAc microgel particles at pH 3.56 (circles) and pH 4.96 (squares). The pH increase induces deprotonation of the AAc groups and hence particle swelling with a concomitant phase transition shift.

SCHEME 1: Equilibrium Hard Sphere Phase Diagram

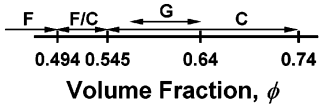

the region where particle concentrations are so low such that particle motion is uncorrelated (gas phase). Instead, the regions relevant to this work, the fluid, crystalline, and glassy phases, are illustrated. Specifically, the fluid phase exists below volume fractions (ϕ) of ∼0.494, where monodispersed hard spheres adopt a state wherein particle motions and positions are correlated, yet no long-range order exists. The freezing point of the system occurs at $\phi = 0.494$, with the melting point being $\phi = 0.545$. Between these two values of ϕ, there exists a phase-separated coexistence between the fluid and crystal phases. Above $\phi = 0.545$ and continuing to the maximum density of $\phi = 0.74$ the thermodynamically preferred state is that of a crystalline assembly, although under many conditions a kinetically trapped jammed or glassy state may result, which is generally considered to exist between $\phi = 0.58$ and $\phi = 0.64$.[14,35] Given this phase behavior, one is inclined to question how particles that deviate strongly from hard spheres might behave and what the ramifications of such dissimilar behaviors are on the assembly of new photonic materials.

To investigate the phase behavior of soft particle assemblies, colloidal crystals were assembled from submicron hydrogel particles composed of the random copolymer pNIPAm-AAc cross-linked (2 mol %) with BIS. As described above, these particles display both pH and temperature responsivity in that the degree of particle swelling is tunable with these stimuli; Figure 1 illustrates this responsivity in the form of temperature-dependent PCS data. This technique allows for determination of the particle translational diffusion coefficient in dilute solution, which can then be converted to a hydrodynamic radius (R_h) via the Stokes−Einstein equation.[36] These data show that below the characteristic VPT temperature the particles are solvent swollen, a state that exists due to favorable hydrogen-bonding interactions between water and the NIPAm amide groups. The temperature responsivity of the particles manifests itself as a large decrease in particle size upon traversing the VPT temperature. This is an entropically favored volume phase transition, where release of water from the polymer network increases the entropy of the system; a concomitant hydrophobic aggregation of the pNIPAm chains occurs thereby resulting in the observed particle size decrease. Although this particular manuscript does not deal directly with the influence of pH on pNIPAm-AAc particle packing, it is worth illustrating the effect pH can have on the particle behavior. Specifically, deprotonation of the AAc groups has a large influence on the degree of swelling. As shown in Figure 1, the particle radius at 25 °C

SCHEME 2: Method of Hydrogel Colloidal Crystal Assembly for Microscope Observation

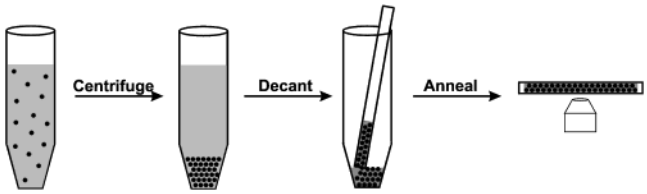

increases from ~410 nm at pH 3.56 to ~530 nm at pH 4.96, reflecting the deprotonation of the AAc groups ($pK_a = 4.25$), which causes an increase in the Donnan potential and osmotic pressure inside the particles.[32,37−40] At pH values further above the pK_a, the particles swell further due to complete deprotonation. However, light scattering data for these particles under those conditions are somewhat unreliable, as the refractive index contrast between the highly swollen particles and the solvent is too small for an adequate scattering intensity to be observed. The ability of the particles to swell in response to pH is illustrative of the chain conformation in the protonated particles. Although the particles are network polymers where the chain conformation is somewhat restricted by cross-links, some degree of a random coil chain conformation is present when the AAc groups are protonated. In other words, the elastic swelling limit of the network does not solely limit the degree of swelling at low pH. However, AAc deprotonation and the resultant increase of the Donnan potential causes the polymer chains to stretch more toward a polyelectrolyte-like (rodlike) conformation and the network is thus swollen toward its elastic limit. As a result of the pH-induced swelling, the magnitude of the size change at the VPT temperature is significantly decreased, as the Coulombic repulsion between neighboring chains decreases the propensity for chain aggregation to occur. This is further evidenced by an increase in the VPT temperature and a broadening of that transition.

Crystal assembly from these particles was accomplished by the method illustrated in Scheme 2. A particle dispersion is first centrifuged to concentrate the particles into a close-packed pellet. Pellets prepared in this fashion are ~6.6% polymer by weight when pNIPAm-AAc copolymer particles are centrifuged at pH 3.8. This viscous polymer mass can then be warmed above the particle VPT temperature to convert the mass into a low-viscosity fluid. A rectangular tube is then inserted into the warm fluid, which then fills the tube by capillary action. After sealing the tube ends to prevent solvent evaporation, the sample is thermally cycled across the VPT temperature to anneal the crystal into a less polycrystalline structure. The dimensions of these tubes are such that crystals formed from ~820 nm diameter particles are >100 lattice planes thick. Figure 2 shows a confocal image taken of a crystal assembled in this fashion from fluorescein-loaded particles. In these samples, the fluorescein was added to the particle solution prior to centrifugation; the water/particle partition coefficient of the fluorescein lies to the side of the particles, thereby providing fluorescence contrast between the particles and the interstices. This image shows that the 111 plane of the face-centered cubic (fcc) lattice assembles at the capillary wall. In general, z-sectioning (not shown) via confocal microscopy shows crystals with either fcc or random hexagonally close-packed (rhcp) structures, depending on the quality of the crystal. Analysis of the image reveals that the average particle center-to-center distance is ~700 nm, indicating that some particle compression may be occurring during packing, as the PCS-determined hydrodynamic diameter is 820 nm. However, it is unwise to ascribe too much quantitative value

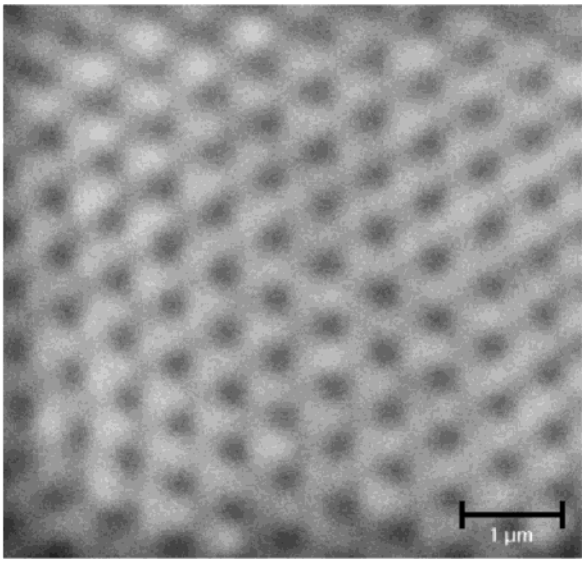

Figure 2. Laser scanning confocal microscopy image of a colloidal crystal assembled from pNIPAm-AAc microgel particles at a polymer concentration of 6.6 wt %. The scale bar is 1 μm.

to these measurements, as the translational diffusion coefficient can be significantly perturbed by dangling chains on the particle surface; the exact relationship between the microscopically observed and spectroscopically determined hydrogel particle sizes is not well-defined. Nonetheless, we have previously demonstrated that large degrees of particle compression are possible in similar materials,[31] so it may indeed be the case that the assembly shown in Figure 2 is comprised of particles that are slightly dehydrated relative to their size in dilute solution. It should further be noted, as we have discussed in previous publications,[30,31] that the thermoresponsivity of the particles allows us to circumvent the kinetically trapped glassy phase during this assembly process. The relatively inelegant and harsh method of assembly used here (centrifugation) would not be expected to yield the thermodynamically preferred particle arrangement, but should instead yield large regions of kinetically trapped glassy phase. However, shrinking the particles by raising the sample above the VPT temperature causes an increase in the particle translational diffusion coefficient (as evidenced by the change in sample viscosity), thereby allowing for assembly of the close-packed thermodynamic product at the expense of the kinetically trapped structure.

To better understand the influence of particle concentration on crystal packing, a series of particle dispersions were prepared over a decade-wide range of concentrations (0.66−6.6 wt % polymer). It is worthwhile noting that these samples were diluted following centrifugation prior to loading into capillaries as opposed to the successive dilution of preformed crystals. Any crystallization observed following dilution should not be the result of any templating or "memory" effects. That is, each sample should represent the thermodynamically preferred phase at that volume fraction and should not be influenced by crystallization that occurred when the system was at a higher concentration. All samples were prepared at a pH of 3.8, where ~75% of the AAc groups are protonated. Furthermore, the ionic strength was held constant at 1 mM, where the Debye−Hückel screening length is <10 nm; electrostatic repulsion should not contribute significantly to packing in these dispersions. Thus, if we consider the highest concentration sample to have a 74% fill fraction, the investigated concentration range should span the hard sphere phase diagram from the crystalline region (ϕ = 0.494 to 0.74) to the fluid region (ϕ = 0.074 to 0.494).

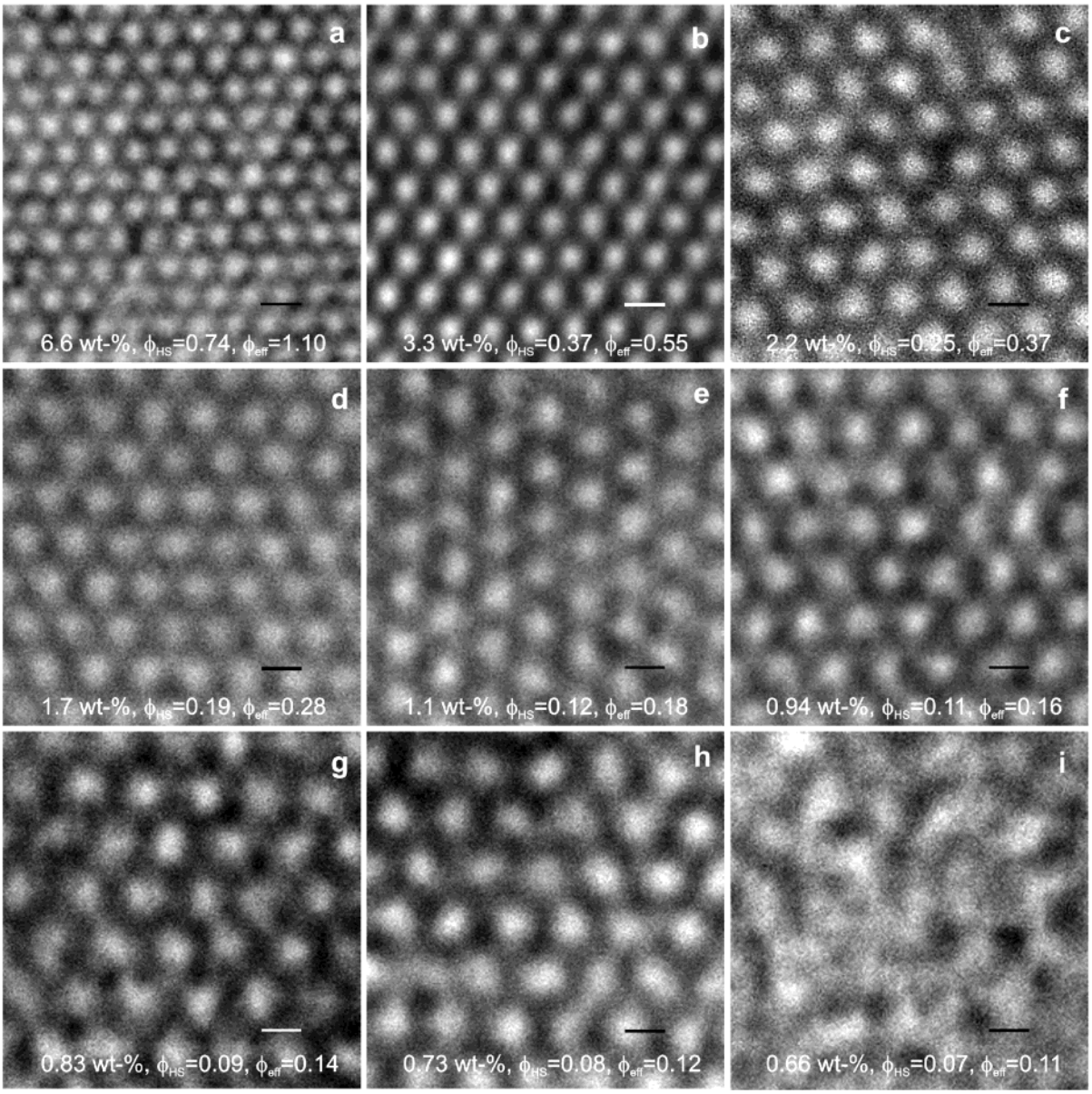

Figure 3. Differential interference contrast microscopy images of colloidal crystals assembled from pNIPAm-AAc microgel particles (R_h = 410 nm). The polymer concentrations in weight percent are indicated on each image, along with the hard sphere (ϕ_{HS}) and effective (ϕ_{eff}) particle volume fractions. See the text for details concerning these values. Scale bars = 1 μm.

Representative images obtained for these samples are shown in Figure 3; the polymer weight percentages are indicated on each image along with the "effective" volume fraction (ϕ_{eff}). This effective volume fraction is estimated from the polymer mass fraction using a treatment previously published by Senff and Richtering.[18,41] In that work, the solvation degree of pNIPAm microgels was determined from rheology measurements as a function of cross-linker concentration and temperature. For example, using their data for ~2 mol % cross-linked pNIPAm particles at 25 °C,[41] one would estimate the ϕ_{eff} for Figure 3a (6.6 wt %) at 1.10 or 110%. The fact that this number is greater than 74% (and indeed, greater than 100%) indicates that the particles have been significantly compressed, as was suggested by the previously presented comparison of the particle sizes obtained from microscopy and PCS. It should be noted that these numbers are simply meant to convey an *estimate* of particle overpacking and hence the "softness" of the particles; it is probable that the absolute magnitude of these estimates are incorrect, given the slightly different synthetic conditions used to produce the microgels used in this study. Also indicated on each panel is the corresponding "hard sphere" particle volume fraction (ϕ_{HS}) that one calculates if Figure 3a is defined as having a volume fraction of 0.74 (close-packed).

An initial overview of this collection of images reveals the surprising result that the particles crystallize spontaneously, even after being diluted 9-fold from the initial polymer concentration (ϕ_{HS} = 0.08, ϕ_{eff} = 0.12, wt % = 0.73, Figure 3h). Indeed, only the highest dilution (10-fold dilution, Figure 3i) shows a disordered fluid phase. If the particles behaved as hard spheres with purely repulsive interaction potentials, the fluid phase should be observable even after a 2-fold dilution (ϕ_{HS} = 0.37, Figure 3b). If we further account for the softness of the particles, melting should at least be observable following a 3-fold dilution (ϕ_{eff} = 0.37, Figure 3c). In a sense, these observations are reminiscent of those related to long-range attractive forces in highly charged colloidal systems.[21−25] In those studies, particle solutions diluted far beyond the theoretically predicted (from DLVO theory) freezing point display an unexpected coexistence

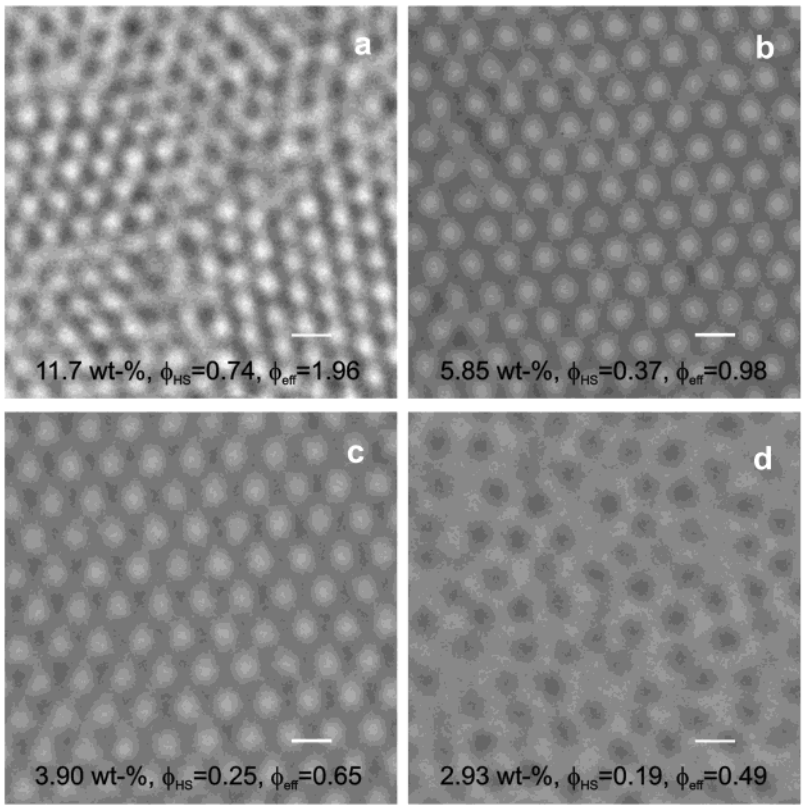

Figure 4. Differential interference contrast microscopy images of colloidal crystals assembled from pNIPAm microgel particles (R_h = 380 nm). The polymer concentrations in weight percent are indicated on each image, along with the hard sphere (ϕ_{HS}) and effective (ϕ_{eff}) particle volume fractions. See the text for details concerning these values. Scale bars = 1 μm.

of crystalline and fluid phases. While the origins of the long-range attractive interactions required for such phenomena remain a matter of debate, it is clear that such effects are typically observed only in highly confined systems and/or with highly charged spheres. Neither condition exists here so it is likely that a different force is influencing packing. Closer inspection of the images in Figure 3 indicates a far more unexpected behavior. In Figure 3a−h, no fluid phase is observable and the particles remain closely packed despite dilution because *the particles themselves have grown in size*. Indeed, in Figure 3h, the center-to-center distance is ∼1.5 μm, which is ∼1.8-times larger than the particle diameter measured in dilute solution by PCS. Although dilution of the dispersion has occurred with respect to polymer wt %, the particles have grown to maximize particle−particle contact, thus maintaining the assembly at a particle volume fraction that is higher than the freezing point. As with the aforementioned phase coexistence studies, our observations can result only from long-range attractive forces in the pair or multibody potential. Since there are no apparent entropic origins of the particle−particle attractive forces, it seems likely that the forces are of enthalpic origin. Examination of the chemical structure and morphology of the pNIPAm-AAc microgel particles suggests that the only possible attractive interactions are AAc-AAc and/or AAc-amide hydrogen bonding between the particles.[42] While it is expected that these interactions would be weak in an aqueous milieu, multiple interactions along the copolymer chain may be sufficient to stabilize the structure. Indeed, the interactions must not be exceedingly strong in this case, because if the particles were excessively "sticky", assembly of the colloidal crystal would be inhibited by particle−particle friction.

A logical test of this hypothesis would be to study assembly as a function of pH, as hydrogen bonding involving AAc is efficient only at pH values below the pK_a of the acid. Above the pK_a, electrostatic repulsion should be dominant. In this case, such experiments do not clearly point to the origin of the effect, however. As described above, raising the pH above the pK_a causes extreme particle swelling and also increases the repulsive forces due to electrostatics. Therefore, similar packing effects may be observed at all pH values, where below the pK_a, hydrogen bonding enforces packing via attractive interactions, while above the pK_a, packing is enforced by electrostatic repulsion and charge-induced particle swelling. As a result of the complications presented by pNIPAm-AAc particles, the hydrogen-bonding hypothesis was tested using pNIPAm particles that do not contain AAc. Again, crystals were prepared by centrifugation of particle dispersions, with all dilutions being performed in the centrifuge tubes prior to capillary loading. In the case of the pNIPAm particles and centrifugation conditions used here, the original (undiluted) pellets were 11.7 wt % polymer as opposed to the 6.6 wt % concentration observed for pNIPAm-AAc. Despite this higher polymer concentration, particle assembly is still observed; the results are shown in Figure 4. Again, both the effective (ϕ_{eff}) and hard sphere (ϕ_{HS}) volume fractions are indicated on each image, along with the wt % polymer in the sample. Analysis of particle packing as a function of volume fraction reveals that efficient packing is observable over a more narrow range of particle concentrations. Image Figure 4a (11.7 wt %, ϕ_{HS} = 0.74, ϕ_{eff} = 1.96) shows a polycrystalline structure in the pNIPAm assembly (R_h = 380 nm by PCS) as was observed for the pNIPAm-AAc system, with the particle center-to-center distance being less than the hydrodynamic diameter, reflecting compression of the particles during centrifugation. Decreasing the particle concentration by a factor of 2 (5.85 wt %, ϕ_{HS} = 0.37, ϕ_{eff} = 0.98, Figure 4b) or three (3.9 wt %, ϕ_{HS} = 0.25, ϕ_{eff} = 0.65, Figure 4c) results in

a crystalline assembly with increased particle spacing. Finally, dilution of the sample by a factor of 4 yields a disordered fluid phase with no evidence of strong particle interactions (2.93 wt %, $\phi_{HS} = 0.19$, $\phi_{eff} = 0.49$, Figure 4d). It is interesting to note that the effective volume fraction of the 4-fold diluted sample lies below the characteristic hard sphere freezing point. It is therefore not surprising that this image should show a fluid phase, since there are no apparent sources of attractive interparticle forces. These results suggest that while microgel particles pack efficiently at high-volume fractions independent of the particle chemistry, the presence of AAc is required for crystal stability over a large range of concentrations. The particle−particle interaction potential is therefore strongly perturbed by the presence of AAc, with the attractive forces likely due to multiple hydrogen-bonding interactions between the microgel particles.

Conclusions

We have demonstrated the assembly of colloidal crystals from poly-*N*-isopropylacrylamide-*co*-acrylic acid microgel particles over a broad range of particle concentrations. At the highest packing density, the particles are overpacked, with the center-to-center distance being smaller than the hydrodynamic diameter as determined by PCS. Dilution of those samples by as much as 9-fold in volume is possible without observation of crystal melting. This broad range of crystalline assembly can only be due to a previously unidentified particle−particle attractive interaction, which causes particle swelling so as to maintain a close-packed structure. The origin of this attractive force is apparently hydrogen bonding between the particles due to AAc dimerization and/or AAc-amide interactions. Hydrogen bonding is further implicated as being the origin of these forces as such attractive forces are apparently absent from particles lacking acrylic acid.

Acknowledgment. L.A.L. gratefully acknowledges support from the Arnold and Mabel Beckman Foundation for a Young Investigator Award and from the Alfred P. Sloan Foundation for a Research Fellowship. We also thank Prof. Mohan Srinivasarao and Dr. Jung O. Park (Georgia Tech, School of Textiles and Fiber Engineering) for assistance with and the use of their confocal microscope.

References and Notes

(1) John, S. *Phys. Rev. Lett.* **1987**, *58*, 2486−2489.
(2) Yablonovitch, E. *Phys. Rev. Lett.* **1987**, *58*, 2059−2062.
(3) Wijnhoven, J.; Vos, W. L. *Science* **1998**, *281*, 802−804.
(4) Vlasov, Y. A.; Yao, N.; Norris, D. J. *Adv. Mater.* **1999**, *11*, 165−169.
(5) Mittleman, D. M.; Bertone, J. F.; Jiang, P.; Hwang, K. S.; Colvin, V. L. *J. Chem. Phys.* **1999**, *111*, 345−354.
(6) Gates, B.; Park, S. H.; Xia, Y. N. *Adv. Mater.* **2000**, *12*, 653.
(7) Sanders, J. V. *Philos. Mag., Part A* **1980**, *42*, 705−720.
(8) Sanders, J. V. *J. Phys., Colloq.* **1985**, 1−8.
(9) Jiang, P.; Bertone, J. F.; Colvin, V. L. *Science* **2001**, *291*, 453−457.
(10) Velev, O. D.; Kaler, E. W. *Adv. Mater.* **2000**, *12*, 531−534.
(11) Hiltner, P. A.; Krieger, I. M. *J. Phys. Chem.* **1969**, *73*, 2386.
(12) Pieranski, P. *Contemp. Phys.* **1983**, *24*, 25−73.
(13) Dinsmore, A. D.; Crocker, J. C.; Yodh, A. G. *Curr. Opin. Colloid Interface Sci.* **1998**, *3*, 5−11.
(14) Pusey, P. N.; van Megan, W. *Nature* **1986**, *330*, 340−342.
(15) Likos, C. N.; Lowen, H.; Watzlawek, M.; Abbas, B.; Jucknischke, O.; Allgaier, J.; Richter, D. *Phys. Rev. Lett.* **1998**, *80*, 4450−4453.
(16) Watzlawek, M.; Likos, C. N.; Lowen, H. *Phys. Rev. Lett.* **1999**, *82*, 5289−5292.
(17) Lowen, H.; Watzlawek, M.; Likos, C. N.; Schmidt, M.; Jusufi, A.; Denton, A. R. *J. Phys.: Condens. Matter* **2000**, *12*, A465−A469.
(18) Senff, H.; Richtering, W. *J. Chem. Phys.* **1999**, *111*, 1705−1711.
(19) Bartsch, E.; Antonietti, M.; Schupp, W.; Sillescu, H. *J. Chem. Phys.* **1992**, *97*, 3950−3963.
(20) Bartsch, E.; Kirsch, S.; Lindner, P.; Scherer, T.; Stolken, S. *Ber. Bunsen-Ges. Phys. Chem.* **1998**, *102*, 1597−1602.
(21) Behrens, S. H.; Grier, D. G. *Phys. Rev. E* **2001**, *64*, 050401/050401−050401/050404.
(22) Grier, D. G. *Nature* **1998**, *393*, 621, 623.
(23) Larsen, A. E.; Grier, D. G. *Nature* **1997**, *385*, 230−233.
(24) Ise, N.; Okubo, T.; Ito, K.; Dosho, S.; Sogami, I. *Langmuir* **1985**, *1*, 176−177.
(25) Ise, N.; Konishi, T.; Tata, B. V. R. *Langmuir* **1999**, *15*, 4176−4184.
(26) Tanaka, T.; Fillmore, D. J.; Sun, S.-T.; Nishio, I.; Swislow, G.; Shah, A. *Phys. Rev. Lett.* **1980**, *45*, 1636−1639.
(27) Pelton, R. *Adv. Colloid Interface Sci.* **2000**, *85*, 1−33.
(28) Saunders, B. R.; Vincent, B. *Adv. Colloid Interface Sci.* **1999**, *80*, 1−25.
(29) Gao, J.; Hu, Z. *Langmuir* **2002**, *18*, 1360−1367.
(30) Debord, J. D.; Lyon, L. A. *J. Phys. Chem. B* **2000**, *104*, 6327−6331.
(31) Debord, J. D.; Eustis, S.; Debord, S. B.; Lofye, M. T.; Lyon, L. A. *Adv. Mater.* **2002**, *14*, 658−661.
(32) Jones, C. D.; Lyon, L. A. *Macromolecules* **2000**, *33*, 8301−8306.
(33) Gan, D.; Lyon, L. A. *J. Am. Chem. Soc.* **2001**, *123*, 7511−7517.
(34) Gan, D.; Lyon, L. A. *J. Am. Chem. Soc.* **2001**, *123*, 8203−8209.
(35) Torquato, S.; Truskett, T. M.; Debenedetti, P. G. *Phys. Rev. Lett.* **2000**, *84*, 2064−2067.
(36) Pecora, R. *Dynamic Light Scattering*; Plenum Press: New York, 1985.
(37) Snowden, M. J.; Chowdhry, B. Z.; Vincent, B.; Morris, G. E. *J. Chem. Soc., Faraday Trans.* **1996**, *92*, 5013−5016.
(38) Flory, P. J. *Principles of Polymer Chemistry*; Cornell University Press: London, 1953.
(39) Fernandez-Nieves, A.; Fernandez-Barbero, A.; Vincent, B.; de las Nieves, F. J. *Macromolecules* **2000**, *33*, 2114−2118.
(40) Ito, S.; Ogawa, K.; Suzuki, H.; Wang, B. L.; Yoshida, R.; Kokufuta, E. *Langmuir* **1999**, *15*, 4289−4294.
(41) Senff, H.; Richtering, W. *Colloid Polym. Sci.* **2000**, *278*, 830−840.
(42) Israelachvili, J. *Intermolecular and Surface Forces*, 2nd ed.; Academic Press: San Diego, 1992.